Malaysian Journal of Mathematical Sciences 2(1): 97-112 (2008)

Characterization of Convexity of Water Bodies

[1]S. Dinesh and [2]A. Pathmanabhan
[1]Science and Technology Research Institute for Defence (STRIDE), Ministry of Defence, Malaysia.
[2] Faculty of Engineering and Technology, Multimedia University
E-mail: dinsat60@hotmail.com

ABSTRACT

Convexity is considered as one the basic descriptors of shapes. In this paper, the characterization of the convexity of water bodies is performed. Concepts of mathematical morphology are used to compare water bodies and their corresponding convex hulls in terms of their size distribution, shape-size complexity and homotopic ratios. A power law relationship is observed between the convexity measures and areas of water bodies. This power law relationship arises as a consequence of the fractal properties of the convexity of water bodies. Convex hull computation increases the size of the water bodies. This enlargement is not even; smaller water bodies undergo smaller enlargements compared to larger water bodies, and hence, convex hull computation alters the water body size distribution. The computed convex hulls have a more even shapiness index distribution compared to the water bodies, as water bodies are random chaotic objects while convex hulls are well defined polygons. Convex hull computation also causes a loss of homotopic information. This study provides useful insight into the dynamical behavior of the floodings of water bodies.

Keywords: water bodies, convexity; water bodies; mathematical morphology; fractal power law relationship; size distribution; shape-size complexity; homotopic ratio.

INTRODUCTION

Convexity is considered as one of the basic descriptors of shapes. Convexity in image processing has been studied for quite some time (Valentine, 1964; Stern, 1989; Boxer, 1993; Held and Abe, 1994; Popov, 1996; Zunic and Rosin, 2004; Rosin and Mumford, 2004; Rahtu et al., 2004, 2006; Kolesnikov and Fränti, 2005; Varošanec, 2007), and has numerous applications, including shape decomposition (Latecki and Lakämper, 1999; Rosin, 2000), camouflage breaking (Tankus and Yeshurun, 2000), object indexing (Latecki and Lakämper, 2000), measurement of border irregularities in medical image analysis (Lee et al., 2003), handwritten word recognition (Kapp et al., 2007) and estimation of derivatives of holomorphic functions (Li, 2007).

An object P is said to be convex if it has the following property: If points A and B belong to P, then all points from the line segment $[AB]$ belong to P as well. The smallest convex set which includes P is called the convex hull of P and is denoted as $CH(P)$. The convexity measure $C(P)$ is defined to be:

$$C(P) = \text{Area } (P) / \text{Area } (CH(P)) \quad (1)$$

Convexity measures have the following properties (Zunic and Rosin, 2004):

1) Convexity measures have the range of (0,1]
2) The convexity measure of a given object equals 1 if and only if this object is convex
3) There are objects whose convexity measure is arbitrarily close to 0
4) The convexity measure of an object is invariant under similarity transformations of the object.

MATHEMATICAL MORPHOLOGY

Mathematical morphology is a branch of image processing that deals with the extraction of image components that are useful for representational and description purposes. Mathematical morphology has a well developed mathematical structure that is based on set theoretic concepts. The effects of the basic morphological operations can be given simple and intuitive interpretations using geometric terms of shape, size and location. The fundamental morphological operators are discussed in Matheron (1975), Serra (1982) and Soille (2003). Morphological operators generally require two inputs; the input image *A*, which can be in binary or grayscale form, and the kernel *B*, which is used to determine the precise effect of the operator.

Dilation sets the pixel values within the kernel to the maximum value of the pixel neighborhood. The dilation operation is expressed as:

$$A \oplus B = \{a + b \; a \in A :, b \in B\} \quad (2)$$

Erosion sets the pixels values within the kernel to the minimum value of the kernel. Erosion is the dual operator of dilation:

$$A \oplus B = \{a + b : a \in A, b \in B\} \tag{3}$$

An opening (Equation 4) is defined as an erosion followed by a dilation using the same kernel for both operation. Binary opening preserves foreground regions that have a similar shape to this kernel, or that can completely contain the kernel, while eliminating all other regions of foreground pixels.

$$A \ominus B = (A^c \oplus B)^c \tag{4}$$

Morphological reconstruction allows for the isolation of certain features within an image based on the manipulation of a mask image X and a marker image Y. It is founded on the concept of geodesic transformations, where dilations or erosion of a marker image are performed until stability is achieved (represented by a mask image) (Vincent 1993).

The geodesic dilation, δ^G used in the reconstruction process is performed through iteration of elementary geodesic dilations, $\delta_{(1)}$ until stability is achieved.

The geodesic dilation δ^G used in the reconstruction process is performed through iteration of elementary geodesic dilations, $\delta_{(1)}$, until stability is achieved.

$$\delta^G(Y) = \delta_{(1)}(Y) \circ \delta_{(1)}(Y) \circ \delta_{(1)}(Y) \ldots \text{until stability} \tag{5}$$

The elementary dilation process is performed using a standard dilation of size one followed by an intersection.

$$\delta_{(1)}(Y) = Y \oplus B \cap X \tag{6}$$

The operation in equation 6 is used for elementary dilation in binary reconstruction. In greyscale reconstruction, the intersection in the equation is replaced with a pointwise minimum (Vincent 1993).

Morphological reconstruction is a useful filtering tool. Figure 1(a) shows an image with circles of various sizes. In order to filter the smaller sized circles, first opening is performed using a square kernel of size 30. The circles that are unable to completely contain the kernel are removed, while

the shape of remaining circles is altered (Figure 1(b)). Morphological reconstruction is implemented with Figure 1(a) being the mask and Figure 1(b) being the marker. This restores the original shape of the remaining circles (Figure 1(c)). This process is known as opening by reconstruction.

CHARACTERIZATION OF CONVEXITY OF WATER BODIES

The data set

Gothavary River, which lies in central India, originates near Triambak in the Nasik district of Maharashtra, and flows through the states of Madhya Pradesh, Karnataka, Orissa and Andhra Pradesh. Although its point of origin is just 80 km away from the Arabian Sea, it journeys 1,465 km to empty into the Bay of Bengal. Some of its tributaries include Indravati, Manjira, Bindusara and Sarbari. Some important urban centers on its banks include Nasik, Aurangabad, Nagpur, Nizamabad, Rajahmundry, and Balaghat. The Gothavary River is often referred to as the Vriddh (Old) Ganga or the Dakshin (South) Ganga. The Gothavary River catchment has an area of 312, 870 km^2 and receives more than 85% of its annual rainfall during the monsoon season (June-September). Hence, the water resource in this river is largely due to monsoon rainfall and largely affected by monsoon extremities, resulting in floods during some years and droughts during others.

Figure 2(a) shows a number of water bodies of varying shape and sizes situated in a portion of the floodplain region of Gothavary River. The water bodies were traced from IRS 1D remotely sensed data. Due to the impracticalities of dealing with incomplete water bodies, only the complete water bodies are considered (Figure 2(b)). A total of 67 distinct individual water bodies (Figure 2(c)) are identified using the connected component labeling (Pitas, 1993).

Computation of convexity measures

The convex hulls of the water bodies (Figure 3) are computed using the convex hull computing neural network (CHCNN) algorithm proposed in Leung et al. (1997). The algorithm is based on a two-layered neural network, topologically similar to ART, with an adaptive training strategy called excited learning. CHCNN provides a parallel on-line and real-time processing of data which, after training, yields two closely related

approximations, one from within and one from the outside, of the desired convex hulls. The accuracy of the approximated convex hull is approximately $O[K^{-1/(n-1)}]$, where K is the number of neurons in the output layer of the CHCNN. When K is taken to be sufficiently large, CHCNN can generate any accurate approximate convex hull.

The convexity measures of the water bodies are computed (Figure 4). It is observed in Figure 5 that the smaller water bodies have larger convexity measures compared to the larger water bodies, indicating that the smaller water bodies have more regularity in terms of their shapes.

A log-log plot of the water body convexity measures C against the water body areas S is drawn (Figure 6). A power law relationship is observed between the two parameters:

$$\log C = 0.1119 * \log S + 0.192 \tag{7}$$

$$C = -0.192 * S^{-0.119} \tag{8}$$

This power law relationship arises as a consequence of the fractal properties of the convexity of water bodies. In Equation 8, 0.192 is a proportionality constant c while 0.119 is the fractal dimension of the convexity of water bodies D, which indicates the distribution of the convexity measures; a higher value of D indicates a more varied distribution, while a lower value of D indicates a more uniform distribution.

Size distribution

Size distribution characterization is performed by implementing opening by reconstruction iteratively on the water bodies and their corresponding convex hulls using square kernels of increasing size. In each iteration, opening removes the objects that are unable to completely contain the kernel. The shapes of the remaining objects are modified. The reconstruction process restores the original shape of the remaining objects.

Plots of the number of objects remaining after each iteration of opening by reconstruction against the kernel size are drawn for the water bodies (Figure 7(a)) and the convex hulls (Figure 7(b)). A well marked peak is observed in Figure 7(a), at kernel size 10. This can be interpreted as the dominant size of the water bodies. The convex hulls have two dominant sizes, at kernel sizes 11 and 13. Significant differences are observed in the plot shapes of Figures 7(a) and 7(b).

These differences occur as convex hull computation enlarges the size of the water bodies, causing changes in their size distribution. This enlargement is not even; as indicated in Figure 5, smaller water bodies undergo smaller enlargements compared to the larger water bodies.

Shape-Size Complexity

The shape-size complexity of the water bodies and their corresponding convex hulls are characterized using the pattern spectrum procedure proposed in Maragos (1989). Pattern spectrum is a shape-size descriptor that is used to detect critical scales in an image object and quantify various aspects of its shape-size content. The term "shape" means any image conveying information about intensity or range, or any other finite-extent signal whose graph is viewed as an image object conveying some pictorial information. The term "scale" is defined as the smallest size of a shape pattern (generated by a kernel) that can fit inside the image.

Pattern spectrum is used to compute the shapiness index of an object, which is the degree of likeness between the object and the kernel used. Shapiness index is computed by first performing recursive opening on the object until all foreground pixels in the image are removed (the image becomes a null set). The shapiness index I of the object is the area of remaining foreground pixels in the image produced one iteration before recursive opening produces a null set $S(Y)$, divided by the area of the original object $S(X)$.

$$I = S(Y)/S(X) \tag{9}$$

A shapiness index value of 1 indicates that the object and the kernel are completely similar. A shapiness index value of 0 indicates that the object and the kernel are geometrically and topologically dissimilar.

The shapiness indices of the water bodies and their corresponding convex hulls are computed using a size 3 square kernel. Plots of the computed shapiness indices against the object areas drawn are drawn for the water bodies (Figure 8(a)) and the convex hulls (Figures 8(b)). It is observed in Figure 8(a) that the smaller water bodies have larger shapiness indices compared to the larger water bodies. The shapiness indices of the convex hulls are more evenly distributed among the larger and smaller convex hulls.

This difference occurs as water bodies consist of chaotic random shapes, while convex hulls are well defined polygons.

Homotopic Ratios

Homotopy is the study of the properties of an object that are unaffected by any deformation, as long as there is no tearing or joining of the object. Homotopic properties are useful for global descriptions of regions in an object plane (Pitas, 1993). A skeleton is a one pixel thick line representation of an object that goes through the middle of the object and preserves the homotopy of the object. Skeletonization is the process of reducing foreground regions in a binary image to a skeleton, while discarding the remaining foreground pixels. The resultant skeleton is used for the computation of length and direction, or for the detection of special topological structures such as end points and triple points (Bookstein, 1979). In this paper, skeletonization is implemented using the skeletonization by morphological thinning algorithm proposed in Jang and Chin (1990). Skeletonization by morphological thinning is defined as successive removal of outer layers of pixels from an object while retaining any pixels whose removal would alter the connectivity or shorten the legs of the skeleton. The process is converged or completed when no further pixels can be removed without altering the connectivity or shortening the skeletal legs.

The homotopic ratios of the water bodies and their corresponding convex hulls are the lengths of the skeletons of the water bodies (Figure 9(a)) divided by the lengths of the skeletons of the convex hulls (Figure 9(b)). A homotopic ratio of 1 indicates that the two objects have completely similar homotopies, while a homotopic ratio of 0 indicates that the two objects have completely dissimilar homotopies. A homotopic ratio of less than 1 indicates a loss of homotopic information, while a homotopic ratio of more than 1 indicates an addition of homotopic information. As shown in Figure 10, all the computed homotopic ratios are less than 1, indicating that convex hull computation causes a loss of homotopic information.

CONCLUSION

In this paper, the characterization of the convexity of water bodies was performed. A power law relationship was observed between the convexity measures and areas of water bodies. This power law relationship arises as a consequence of the fractal properties of the convexity of water

bodies. Convex hull computation increases the sizes of the water bodies. This enlargement is not even; smaller water bodies undergo smaller enlargements compared to larger water bodies, and hence, convex hull computation alters the water body size distribution. The computed convex hulls have a more even shapiness index distribution compared to the water bodies, as the water bodies are random chaotic objects while convex hulls are well defined polygons. Convex hull computation also causes a loss of homotopic information.

In general, water bodies have varying degrees of convexity, while the self organized criticalities of their floodings are convex objects. The study of the convexity of water bodies can provide useful insight into the flooding properties of water bodies. Work is currently being done to study the convexity of various degrees of simulated floodings.

REFERENCES

A. Held and K. Abe. 1994. On approximate convexity. Pattern Recog. Lett., **15(6)**:611-618.

A. Kolesnikov and P. Fränti. 2005. Optimal algorithm for convexity measure calculation. *IEEE International Conference on Image Processing 2005 (ICIP 2005),* 353-356.

A.T. Popov. 1996. Fuzzy morphology and fuzzy convexity measures. *Proc. 13th International Conference on Pattern Recognition,* **2**: 611-614.

B.K. Jang and R.T. Chin. 1990. Analysis of thinning algorithms using mathematical morphology. *IEEE Trans. Image Process*., **12(6)**: 541-550.

E. Rahtu, M. Salo and J. Heikklä. 2006. A new convexity measure based on a probabilistic interpretation of images. *IEEE Trans. Image Process*., **28(9):**1501 – 1512.

E. Rahtu, M. Salo and J. Heikklä. 2004. Convexity recognition using multiscale autoconvolution. *Proc. 17th International Conference on Pattern Recognition,* **1**: 692-695.

F.L. Bookstein. 1979. The line skeleton. *Comput. Vision Graph*., **11(2)**: 123-137.

F. Valentine. 1964. *Convex Sets*. McGraw Hill, San Francisco.

G. Matheron. 1975. *Random Sets and Integral Geometry*. New York, Wiley.

H.I Stern. 1989. Polygonal entropy: A convexity measure. *Pattern Recog. Lett*., **10**: 229-235.

I. Pitas. 1993. *Digital Image Processing Algorithms*. Prentice Hall, London.

J.L. Li. 2007. Estimates for derivatives of holomorphic functions in a hyperbolic domain. *J. Math. Anal. Applic*., **329(1):**581-591.

J. Serra. 1982. *Image Analysis and Mathematical Morphology*. Academic Press, London.

J. Zunic and P.L. Rosin. 2004. A new convexity measure for polygons. *IEEE Trans. Image Process*., **27(7):** 923-934.

L. Boxer. 1993. Computing deviations from convexity in polygons. *Pattern Recog. Lett.,* **14(3)**: 163-167.

L.J. Latecki and R. Lakämper. 1999. Convexity rule for shape decomposition based on discrete contour evolution. *Comput. Vision Image Und.,* **73(3)**:441-454.

L.J. Latecki and R. Lakämper. 2000. Shape similarity measure based on correspondence of visual parts. *IEEE Trans. Image Process.*, **22(10):**1185-1190.

L. Vincent. 1993. Morphological reconstruction in image analysis: applications and efficient algorithms. *IEEE Trans. Image Process.,* **2 (2):** 176-201.

M.N. Kapp, C.O.A Freitas, and R. Sabourin. 2007. Methodology for the design of NN-based month-word recognizers written on Brazilian bank checks. *Image Vision Comput.*, **25(1):** 40-49.

P.L. Rosin. 2000. Shape partitioning by convexity. *IEEE T. Syst. Man Cy. A*, **30(2)**: 202-210.

P.L Rosin and C.L. Mumford. 2004. A symmetric convexity measure. *Proc. 17th International Conference on Pattern Recognition*, **4**: 11-14.

P. Maragos. 1989. Pattern spectrum and multiscale shape representation. *IEEE Trans. Image Process.*, **11(7)**: 701-716.

P. Soille. 2003. *Morphological Image Analysis: Principles and Applications*. Springer Verlag , Berlin.

S. Varošanec. 2007. On h-convexity. *J. Math. Anal. Applic.*, **326 (1)**: 303-311.

T.K. Lee and D. McLean and M.S. Atkins. 2003. Irregularity index: A new border irregularity measure for cutaneous lesions. *Med. Image Anal.,* **7(1):** 47-64.

Y. Leung, J.S. Zhang and Z.B. Xu. 1997. Neural networks for convex hull computation. *IEEE T. Neural Networ.,* **8(3):** 601-611.

FIGURES

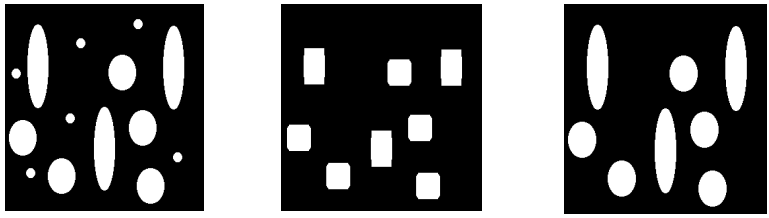

(a) The original image (b) The opened image (c) The reconstructed image

Figure 1: Application of opening by reconstruction to perform filtering.

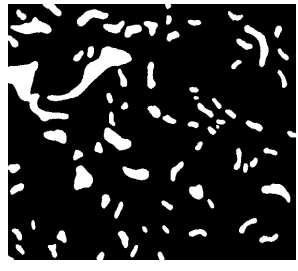

(a) The original water bodies traced from IRS 1D remotely sensed data

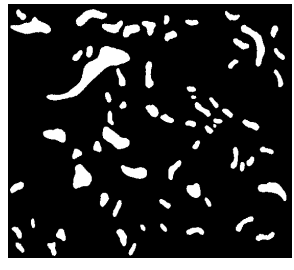

(b) The water bodies after removal of incomplete water bodies

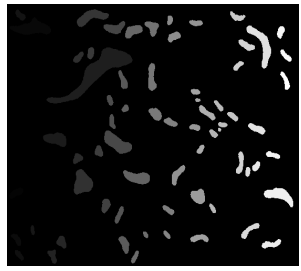

(c) Identification of the individual water bodies using connected component labeling. The water body count number is determined by the grey level; the brighter the grey level, the larger the water body number.

Figure 2: Water bodies of varying shape and sizes situated in a portion of the flood plain region of Gothavary River.

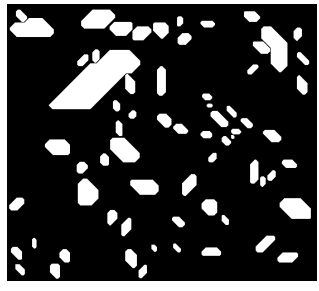

Figure 3: The convex hulls of the water bodies.

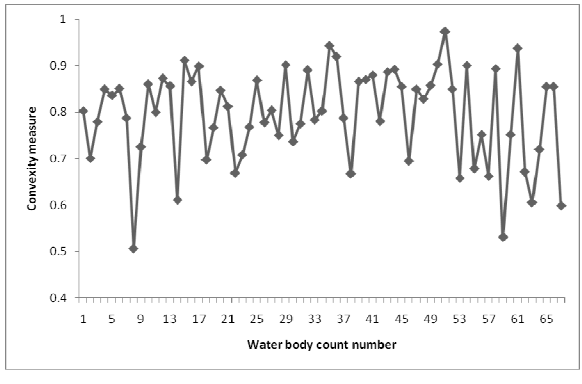

Figure 4: Convexity measures of the water bodies.

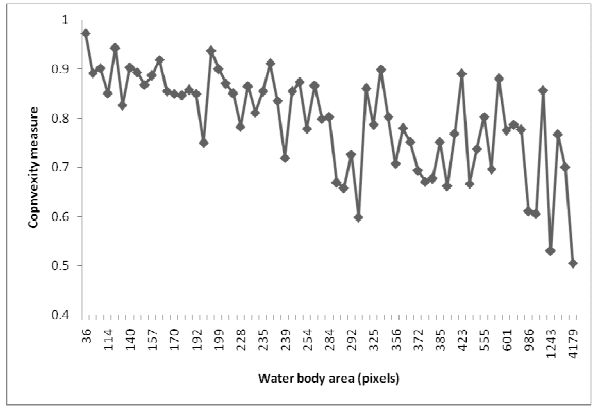

Figure 5: Plot of the convexity measures against the areas of the water bodies.

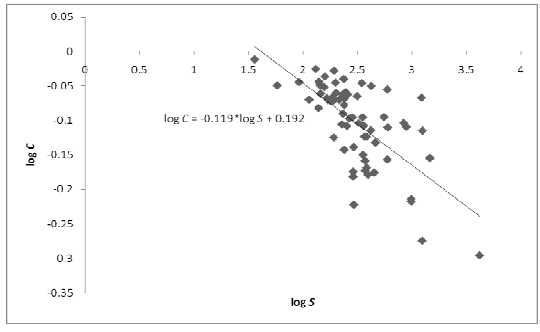

Figure 6: Log-log plot of the convexity measures C against the areas of the water bodies S.

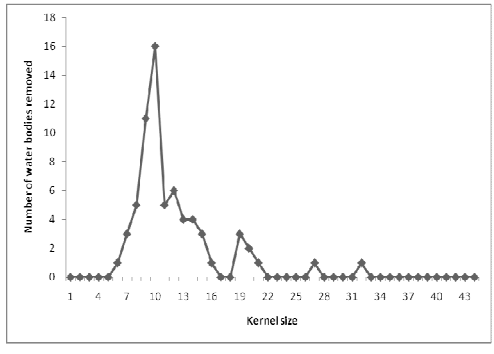

(a) The water bodies

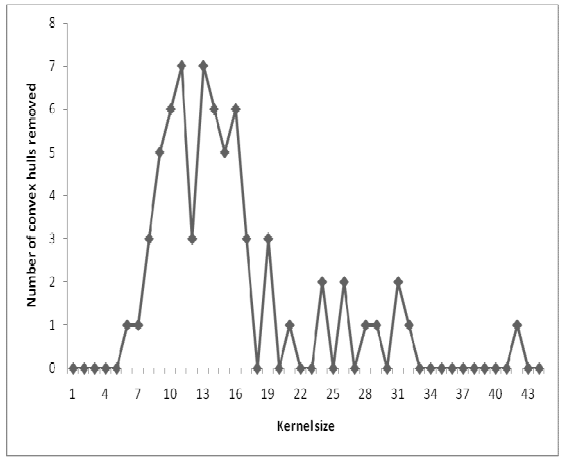

(b) The convex hulls.

Figure 7: Plots of the number of objetcs remaining after each interation of opening by reconstruction against kernel size

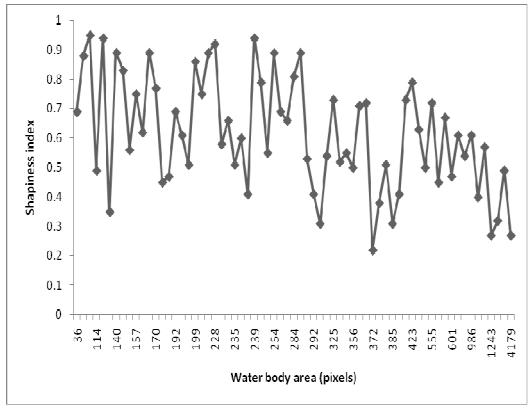

(a) The water bodies

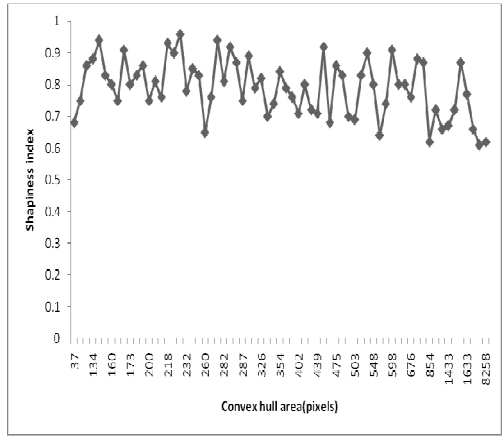

(b) The convex hulls

Figure 8: Plots of the shapiness indices against the areas of the objects

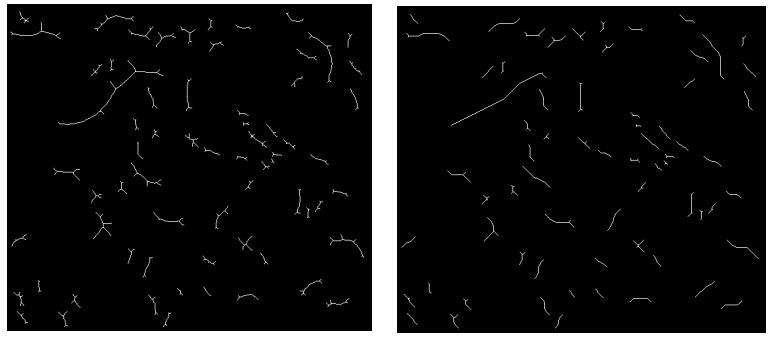

(a)The water bodies (b) The convex hulls

Figure 9: Skeletons

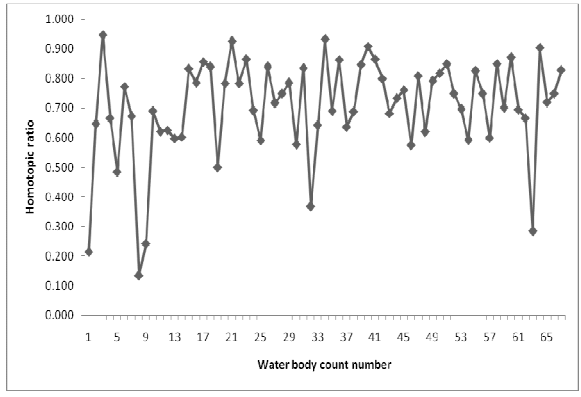

Figure 10: Homotopic ratios of the water bodies and their corresponding convex hulls.